Article

Not peer-reviewed version

The EnvC Homolog Encoded by Xanthomonas citri subsp. citri Is Necessary for Cell Division and Virulence

Michelle M. Pena , Thaisa Z. Martins , Doron Teper , Caio Zamuner , Helen Alves Penha , Henrique Ferreira , Nian Wang , Maria Inês T. Ferro , Jesus A. Ferro *

Posted Date: 12 October 2023

doi: 10.20944/preprints202310.0767.v1

Keywords: citrus canker; hydrolase; periplasmic protein; cell division

Article

The EnvC Homolog Encoded by *Xanthomonas citri* subsp. *citri* Is Necessary for Cell Division and Virulence

Michelle M. Pena [1$#], Thaisa Z. Martins [1#], Doron Teper [2], Caio Zamuner [3], Helen Penha [4], Henrique Ferreira [3], Nian Wang [5], Maria Inês T. Ferro [4] and Jesus A. Ferro [4,*]

[1] Agricultural and Livestock Microbiology Graduation Program, São Paulo State University (UNESP), School of Agricultural and Veterinarian Sciences, Jaboticabal, SP, Brazil; mpmaclellan@uga.edu (M.M.P.); thaisazmartins@gmail.com (T.Z.M.)

[2] Department of Plant Pathology and Weed Research, Institute of Plant Protection Agricultural Research Organization (ARO), Volcani Institute, Rishon LeZion, Israel; doront@volcani.agri.gov.il (D.T.)

[3] Biochemistry Building, Institute of Biosciences, São Paulo State University (UNESP), Rio Claro, 13.506-900, SP, Brazil; c.zamuner@unesp.br (C.Z.); henrique.ferreira@unesp.br (H.F.)

[4] Department of Agricultural, Livestock and Environmental Biotechnology, São Paulo State University (UNESP), School of Agricultural and Veterinary Sciences, Jaboticabal, SP, Brazil; helen.penha@unesp.br (H.P.); maria.ferro@unesp.br (M.I.T.F.); jesus.ferro@unesp.br (J.A.F.)

[5] Citrus Research and Education Center, Department of Microbiology and Cell Science, Institute of Food and Agricultural Sciences, University of Florida, Lake Alfred, U.S.A.; nianwang@ufl.edu (N.W.)

[$] Current address: Department of Plant Pathology, University of Georgia, Tifton, GA, U.S.A

[*] Correspondence: jesus.ferro@unesp.br

[#] These authors contributed equally to this manuscript.

Abstract: Peptidoglycan hydrolases are enzymes that cleave the peptidoglycan of the bacterial cell wall, facilitating cell growth, cell division, and peptidoglycan turnover. *Xanthomonas citri* subsp. *citri* (*X. citri*), the causal agent of citrus canker, encodes an *Escherichia coli* M23 peptidase EnvC homolog. EnvC is a LytM factor required for septal peptidoglycan splitting and daughter cell separation. In this study we investigate how EnvC contributes to the virulence and cell separation of *X. citri*. We observed that disruption of the *X. citri envC* gene (Δ*envC)* led to a reduction in virulence. Upon inoculation into leaves of Rangpur lime (*Citrus limonia* Osbeck), the *X. citri* Δ*envC* mutant showed a delay in causing citrus canker symptoms compared with the wild-type *X. citri* strain. Mutant complementation restored the *X. citri* wild type phenotype. Subcellular localization confirmed that *X. citri* EnvC is a periplasmic protein. Moreover, the *X. citri* Δ*envC* mutant exhibited elongated cells, indicative of a cell division defect. These findings support the role of EnvC in regulating virulence, cell wall organization, and cell division in *X. citri*.

Keywords: citrus canker; hydrolase; periplasmic protein; cell division

1. Introduction

Xanthomonas citri subsp. *citri* (*X. citri*) is a phytopathogenic Gram-negative bacterium and the causal agent of citrus canker, a severe disease that affects all economically important citrus varieties worldwide [1], causing significant economic losses. Gram-negative bacteria possess a tight peptidoglycan (PG) layer located in the periplasmic space between their outer and inner membranes [2]. This polymer is composed of glycan strands of β-1,4-glycosidic bond-linked N-acetylglucosamine (GlcNAc) and N-acetylmuramic acid (MurNAc) disaccharides, which are cross-linked by short peptides and play an essential role in the preservation and maintenance of cell shape and cell integrity [3]. Two main classes of peptidoglycan-lytic enzymes are responsible for the PG's assembly: the glycosidases that cleave the glycan backbone and the amidases (or peptidases) that cleave the peptide sidechain [4]

 doi:10.20944/preprints202310.0767.v1

The *X. citri* strain 306 (GenBank AE008923.1) possesses nine proteins sharing the peptidase M23 domain, and four of them are hypothetical proteins with no function described so far (Supplementary Table S1). One of these proteins, XAC0024 (GenBank AAM34916.1), is a homolog of EnvC in *E. coli*, a protein widely distributed in bacteria [5]. EnvC is highly conserved within Gram-negative bacteria and functions as part of the septal ring apparatus [6]. In *E. coli*, EnvC is a periplasmic peptidase that plays a role in septal peptidoglycan splitting and daughter cell separation [7]. Deletion of the E. coli *envC* gene, like other genes encoding LytM domain hydrolases such as *nlpD*, *ygeR*, and *uebA*, leads to the formation of long cell chains, suggesting a defect in cell separation [7]. It was demonstrated that EnvC controls cell separation by activating PG-degrading amidases AmiA and AmiB [8]. Homologs of *envC* have been shown to perform similar functions in multiple bacterial species and are essential for the pathogenicity of several animal bacterial pathogens, including *Vibrio cholera*, enterohemorrhagic *E. coli*, and *Fusobacterium nucleatum* [9,10,11]. The *envC* homolog of *Pseudomonas aeruginosa* was identified to be functionally redundant to *nlpD*, as deletion of both led to the formation of long cell chains and enhanced sensitivity to high temperature and antimicrobial compounds [12].

The role of LytM factors and PG amidases in pathogenicity and cell division was recently characterized in *X. campestris* pv. *campestris* [13]. Deficiency in cell separation was observed in either *nlpD* or *envC* deletion strains; however, the deletion of the single gene *nlpD* had a significant effect on virulence and induction of the hypersensitive response in non-host plants, while deletion of *envC* did not significantly affect host interactions [13].

In the present study, we characterized the *envC* homolog (XAC0024) of *X. citri* strain 306. We found that *envC* is essential for virulence but did not completely compromise the ability of *X. citri* in triggering weak symptoms in a susceptible host genotype. Also, *X. citri* Δ*envC* displayed an altered cell shape compared to the wild-type strain. Similar to what was observed for other Gram-negative bacteria, *X. citri envC* gene seems to play a role in daughter cell separation. Moreover, the subcellular localization of *X. citri* EnvC protein linked to mCherry fluorophore (EnvC-mCherry) is consistent with the protein occupying the periplasmic region.

2. Materials and Methods

2.1. Bacterial strains, plasmids, and culture condition

The bacterial strains and plasmids used in the present work are listed in Table 1. *Escherichia coli* (*E. coli*) strains DH10B, SM10λpir, and HST08 – Stellar used for cloning were cultivated at 37℃ in LB/LB-agar medium [14]. Growth in liquid medium was at 250 rpm (shaker) for 14-16 h and growth in solid medium was in a bacteriological incubator for 14-16 h. *Xanthomonas citri* subsp. *citri* (*X. citri*) 306 strain were cultivated at 30℃ in NYG-rich medium (3 g/L yeast extract, 5 g/L peptone, 20 g/L glycerol, pH 7.0), NB medium ("Nutrient Broth": 3 g/L meat extract, 5 g/L peptone), or on NB-agar plates (NB medium containing 15 g/L agar), supplemented with L-arabinose (0.05% w/v), starch (0.2% w/v), and sucrose (5% w/v) when required. Growth in liquid medium was at 250 rpm (shaker) and growth in solid medium was in a bacteriological incubator for 48 h. The antibiotics carbenicillin and kanamycin or ampicillin and spectinomycin were used when required, at the concentration of 50 μg/mL and 100 μg/mL, respectively.

Table 1. List of strains and plasmids used in this work.

Strains	Characteristics	References
X. citri 306	*Xanthomonas citri* subsp. *citri* strain 306 (wild-type strain)	IBSBF 1594; [15]
Δ*envC*	*X. citri envC* deletion mutant (deletion of genomic bases 26156 to 26748)	This work
E. coli DH10B	Cloning strain	Invitrogen, Waltham, MA, USA
E. coli SM10λpir	Cloning strain	Laboratory Stock

 doi:10.20944/preprints202310.0767.v1

E. coli HST08	Cloning strain	Takara Bio USA, Inc. Mountain View, CA, USA
Plasmids	**Characteristics**	**References**
pGEM® -T easy	Cloning vector; Ap^R	Promega
pOK1	*sacB-sacR*; Sp^R	[16]
pMAJIIc	Derivative of pGCD21; mCherry expression vector; Ap^R; Neo^R/Km^R; *ara*C-p*ara;* integrative vector in *X. citri*;	[17] (GenBank MT119765)

Ap^R: ampicillin resistance; Km^R: kanamycin resistance; Neo^R: neomycin resistance; Sp^R: spectinomycin resistance.

2.2. Mutant construction

2.2.1. Partial deletion of XAC0024 nucleotide sequence

The *X. citri* strain containing the disrupted XAC0024 gene (mutant Δ*envC*) was obtained through site-directed mutagenesis using the overlap extension approach in the polymerase chain reaction [18]. To construct the XAC0024 mutant, *X. citri* genomic DNA was used as a template in two-step PCR reaction. In the first step, the primers A(F) and B(R), and C(F) and D(R) (Supplementary Table S2) were used in two separate reactions to generate fragments AB and CD, respectively, which were then linked through a double-joint PCR. The PCR reaction, in a final volume of 20 µL, contained 26.5 ng of DNA, 0.2 mM of each dNTP, 1U of Phusion High Fidelity DNA Polymerase (New England Biolabs), 0.5 µM of each primer, and 3% of DMSO for primer pairs A-B and 5% of DMSO for primer pairs C-D. The PCR conditions were as follows: 98°C for 30s, 35 cycles of 98°C for 10s, 69°C for 30s, and 72°C for 30s, with a final extension at 72°C for 10 min, in a Veriti® 96-Well Thermal Cycler (Applied Biosystems). The PCR products were purified using the Kit Wizard® SV Gel and PCR Clean-Up System (Promega) and quantitated using the NanoDrop® ND-1000 spectrophotometer (Thermo Fisher Scientific). The size of the amplified fragments AB and CD was confirmed by agarose gel electrophoresis (Supplementary Figure S1). The double-joint PCR step was performed using fragments AB and CD as templates and the primers A(F) and D(R) to generate the A-D fragment, using 3% DMSO and the same PCR conditions described before, except that the final volume was 50 µL. The amplified product was subjected to 0.7% agarose gel electrophoresis, and the band with the expected size was recovered from the gel using the Kit Wizard® SV Gel and PCR Clean-Up System (Promega). The purified DNA fragment was quantitated in a NanoDrop® ND-1000 spectrophotometer (Thermo Fisher Scientific) and submitted to a PCR reaction to add a 3'-A overhang to the ends of the AD fragment using a final concentration of 0.2 mM dATP and 1 U of Platinum® Taq DNA Polymerase Recombinant (Invitrogen) in a final volume of 50 µL in a 10-min reaction at 72°C in a GeneAmp® PCR System 9700 (Applied Biosystems).

2.2.2. Deletion vector construction

The PCR-amplified AD fragment containing 3'-A overhangs was ligated into plasmid pGEM®-T Easy (Promega) using T4 DNA ligase according to the manufacturer's instructions. The ligation reaction contained 50 ng of plasmid, 118 ng of insert, in a final volume of 10 µL. Then, an aliquot of 2 µL of the ligation reaction was used to transform 50 µL of chemically competent *E. coli* DH10B cells (Invitrogen) following the protocol described by [14]. The recombinant bacteria carrying the plasmid DNA harbouring the A-D fragment were selected by plating onto agar plates containing solid LB medium, 100 µg/mL of ampicillin, 0.1 mM of IPTG (Isopropyl-β-D-1-thiolgalactopyranoside) and 0.0032% of Xgal (5-bromo-4-chloro-3-indolyl-β-D-galactoside). After incubation at 37°C for 16 h, two white colonies were picked and their recombinant plasmid was isolated using the Wizard® Plus SV Minipreps DNA Purification System (Promega) following the manufacturer's instructions. The presence of the A-D fragment was checked by PCR using the vector primers M13/pUC F-20 and M13/pUC R-48 (Table S1), and the sequence was confirmed by sequencing on an ABI 3730xl DNA

 doi:10.20944/preprints202310.0767.v1

analyzer (Applied Biosystems) using the same vector primers. Next, the recombinant plasmid was digested with *ApaI* and *SalI* restriction enzymes (New England Biolabs), and the A-D fragment was recovered from an agarose gel as described before. Subsequently, it was ligated into the suicide pOK1 plasmid previously digested with the same enzymes. The ligation reaction was used to transform chemically competent *E. coli* SM10 ◎pir cells to the protocol described by [14]. The recombinant bacteria carrying the recombinant pOK1 plasmid were selected by plating them onto agar plates containing solid LB medium and 100 µg/mL of spectinomycin. The pOK1 plasmid DNA was purified using the kit Wizard® Plus SV Minipreps DNA Purification System (Promega), and the presence of A-D fragment was confirmed by PCR using A(F) and D(R) primers.

2.2.3. Mutant obtention

The pOK1 suicide vector carrying the A-D sequence from XAC0024 was used to delete the bases 370 to 962 of the XAC0024 gene (1236 bp) by integrating the suicide vector into chromosomal DNA via double-crossover homologous recombination. Electrocompetent *X. citri* 306 wild-type (wt) cells were transformed with recombinant pOK1 vector as described by [19]. The screening of the deletion mutant followed the methodology described by [20], using NB-agar medium with the addition of spectinomycin antibiotic. Since pOK1 vector has the *SacB* gene, positive selection for the loss of the vector was achieved by growth on sucrose. Colonies that grew in sucrose but not in the presence of spectinomycin were selected, and their genomic DNA was extracted using the Wizard® Genomic DNA Purification Kit (Promega), according to the manufacturer's instructions. The deletion was confirmed by PCR reaction using 50 ng of mutant and *X. citri* 306 wt genomic DNAs, GoTaq® DNA Polymerase, primers A(F) and D(R). The amplicons were visualized in a 1% agarose gel, and the ones with the expected length were then sequenced, and the confirmed mutant was named *X. citri* Δ*envC* (Δ*envC*).

2.3. Mutant complementation

For the complementation of the Δ*envC* mutant, a fragment of 2236-bp comprising the genome region from 25382 to 27617 bases, containing 1236-bp of the ORF XAC0024 plus 500 bp upstream of the 5′ end and 500 bp downstream of the 3′ end, was amplified using the primers 0024_500_IF_F / 0024_500_IF_R (Supplementary Table S2) and Q5 High-Fidelity DNA Polymerase (New England Biolabs). The PCR-amplified fragment was ligated into the *Xho*I site of pMAJIIc plasmid [17] using the *In-Fusion HD Cloning Kit* (Takara Bio USA, Inc.) as recommended by the manufacturer. The complementation plasmid was confirmed by DNA sequencing (primer XAC0024_mcherry_F – Supplementary Table S2) and used to transform the *X. citri* Δ*envC* strain to produce *X. citri* Δ*envC* pMAJIIc-*envC (X. citri* Δ*envC amy*:pMAJIIc-*envC).*

2.4. Subcellular localization

2.4.1. Vector construction

For the construction of the plasmid pMAJIIc-*envC* that enables the subcellular localization of proteins fused to mCherry fluorescent protein, the *X. citri envC* gene (XAC0024) sequence was PCR amplified with the primers 0024_IF_F and 0024_IF_R (Supplementary Table S2) using *X. citri* 306 genomic DNA as a template, and ligated into the *Xho*I site of pMAJIIc plasmid [17] using the *In-Fusion HD Cloning Kit* (Takara Bio USA, Inc.) as recommended by the manufacturer. The plasmid construction was confirmed by DNA sequencing (primers pGCD21-F and XAC0024_mcherry-F – Supplementary Table S2) and used to transform electrocompetent *X. citri* 306 strain cells to produce the *X. citri* pMAJIIc-*envC* (*X.citri amy*::pMAJIIc-*envC*) strain.

2.4.2. Fluorescence Microscopy

Starting cultures of *X.citri* wt and *X. citri* pMAJIIc-*envC* were prepared by cultivating bacteria in 5.0 mL of NB medium for approximately 16 hours at 30℃ and 200 rpm. The cultures were then

 doi:10.20944/preprints202310.0767.v1

diluted to an OD 600 nm of 0.1 using fresh NB medium for a final volume of 5.0 mL and subsequently cultivated under the same conditions until an OD 600 nm of 0.3 was reached. At this point, arabinose was added to the medium to a final concentration of 0.05% and the cultures were kept at 30°C and 200 rpm. After a minimum of two hours of induction, drops of 5 µL of cell cultures were placed on agarose-covered microscope slides for direct microscope observation [21]. For chromosome visualization, *X.citri* wt, Δ*envC* and Δ*envC* pMAJIIc-*envC* cells were cultivated under the same conditions described above and stained with DAPI using the protocol described by [22]. Bacteria were visualized using an Olympus BX61 microscope equipped with a monochromatic OrcaFlash2.8 camera (Hamamatsu, Japan) and TxRed and DAPI filters. Data collection and analysis were performed with the software CellSens Version 11 (Olympus). Statistical analyses were conducted using GraphPad Prism version 6.

2.5. Pathogenicity and bacterial viability analyses

Pathogenicity tests were conducted in triplicate using Rangpur lime (*Citrus limonia*) as the plant host. Bacterial cultures (*X. citri wt*, Δ*envC* and Δ*envC* pMAJIIc-*envC*) were adjusted to 10^8 CFU/mL (OD 600 nm of 0.3) using sterile 0.9% NaCl solution, and then inoculated on the abaxial surface of leaves using a needleless syringe. The negative control consisted of inoculating with sterile 0.9% NaCl solution. Inoculated plants were kept in a controlled environmental plant laboratory equipped with an HEPA filter to maintain air particle purity. The conditions were set at 28–30℃, 55% humidity, and a 12-hour light cycle and the plants were observed for up to 30 days to monitor the appearance of citrus canker symptoms. Photos were taken at the 3rd, 5th, 7th, 10th, 12th, and 15th DAI (days after inoculation).

2.6. Growth curves

X. citri wt, Δ*envC* and Δ*envC* pMAJIIc-*envC* were initially cultivated in NB medium for 16 h at 30℃ and 200 rpm. For the *in vitro* growth curves, cultures were subsequently diluted in fresh NB medium to an OD 600nm of 0.1 in a final volume of 1.5 mL (OD 600 nm of 0.3 corresponds to 10^8 CFU/mL). Cell cultures were then distributed in the wells of a 24-wells microtiter plate and incubated in a microtiter plate reader (Synergy H1N1; BioTek) at 30℃ with constant agitation (200 rpm) and the OD at 600 nm was measured every 30 min for 72 hours [23]. For the *in planta* growth curves, bacterial cultures of *X. citri* wt and Δ*envC* in NB medium were adjusted to 10^6 CFU/mL with ultrapure water and infiltrated into the abaxial surface of leaves of Rangpur lime (*Citrus limonia*) using a needleless syringe. The inoculated plants were kept in the controlled environment plant laboratory described before. Samples for colony counting were obtained by collecting 1 cm^2 leaf discs from the inoculation point at 0, 1, 3, 6, 10, 15, 20 and 25 DAI, and the leaf discs were macerated in 1.0 mL of 1x PBS buffer (NaCl 8 g/L, KCl 0.2 g/L, Na_2HPO_4 1.44 g/L and KH_2PO_4 0.24 g/L, pH 7.4) in sterile 1.5 mL Eppendorf tubes with a plastic sterile pestle. After a serial dilution by factors of 10, ranging from 10^{-1} to 10^{-6}, three aliquots of 50 µL for each dilution were plated on NB-agar medium plates for colony counting.

2.7. Phylogenetic analyses and protein modeling

A single gene alignment based on the XAC0024 gene sequence and the recovered sequences from different species of *Xanthomonas* (Table S3) were performed using ClustalW [24]. For probabilistic analyses, the best evolutionary model was determined using jModelTest performed on the CIPRES resource [25]. Maximum Likelihood analyses (ML) were conducted with RAxML version 8.0.24 [26] and the branch support was assessed using bootstrap analysis [27] with 1000 replicates. The cladogram was drawn using MEGA X software [28].

For protein modeling, the 'Threading ASSEmbly Refinement' (I-TASSER) program [29] was utilized to access and compare the 3-D structures of the proteins XAC0024 from *X. citri* 306 and the protein EnvC from *E. coli*. The protein sequence of XAC0024 was retrieved from the *Xanthomonas* sp. database [30], and the protein sequence of EnvC from *E. co*li was retrieved from NCBI [31].

Preprints (www.preprints.org) | NOT PEER-REVIEWED | Posted: 12 October 2023 doi:10.20944/preprints202310.0767.v1

3. Results

3.1. X. citri encodes an EnvC homolog that is conserved in many bacteria

The protein XAC0024 is highly conserved in other sequenced *Xanthomonas* species, as shown by the Maximum Likelihood tree (Figure 1). Although the single gene used in the reconstruction does not reflect the known phylogeny for the *Xanthomonas* genus, based on the core genome alignment [32], it was possible to recover some expected clusters. The *X. citri* and *X. fuscans* species showed a close relationship and, together with *X. axonopodis* and *X. euvesicatoria* (*X. campestris 85-10*), formed the clade "*X. axonopodis*" [33]. The clade constituted by the species *X. arboricola*, *X. fragariae*, *X. hortorum* and *X. gardneri* was consistent with the clade A topology in [32], having *X. hortorum* and *X. gardneri* species forming a tight cluster [34].

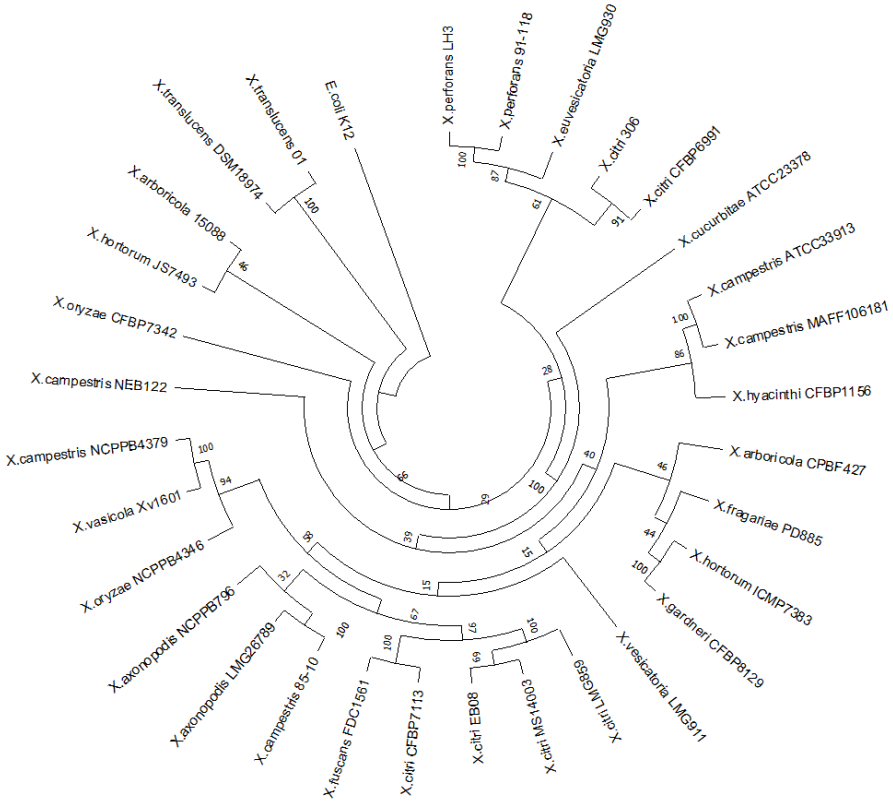

Figure 1. Maximum Likelihood phylogeny based on the nucleotide sequences of 31 strains representing the *Xanthomonas* genus.

The nucleotide sequence comparison between XAC0024 from *X. citri* 306 and the recently published homolog XCC0022 from *X. campestris* pv. *campestris* str. ATCC 33913, showed an identity of 85% (Figure S2). Further analysis of the protein sequences revealed that XAC0024 and XCC0022 shared an identity of 89%, a coverage of 98%, and a similarity of 93% (Figure S3). These findings indicate a considerable level of sequence conservation between the two proteins. To explore the shared conserved domains among these proteins, we utilized the NCBI Batch Web CD-Search tool. Figure 2 displays the visualization of the identified conserved domains between the three protein sequences from *X. citri* 306 (XAC0024), *X. campestris* (XCC0022), and *E. coli* (EnvC) (See Supplementary Figure S4 for a detailed visualization of the nine ORFs of *X. citri* sharing the M23 domain).

Preprints (www.preprints.org) | NOT PEER-REVIEWED | Posted: 12 October 2023 doi:10.20944/preprints202310.0767.v1

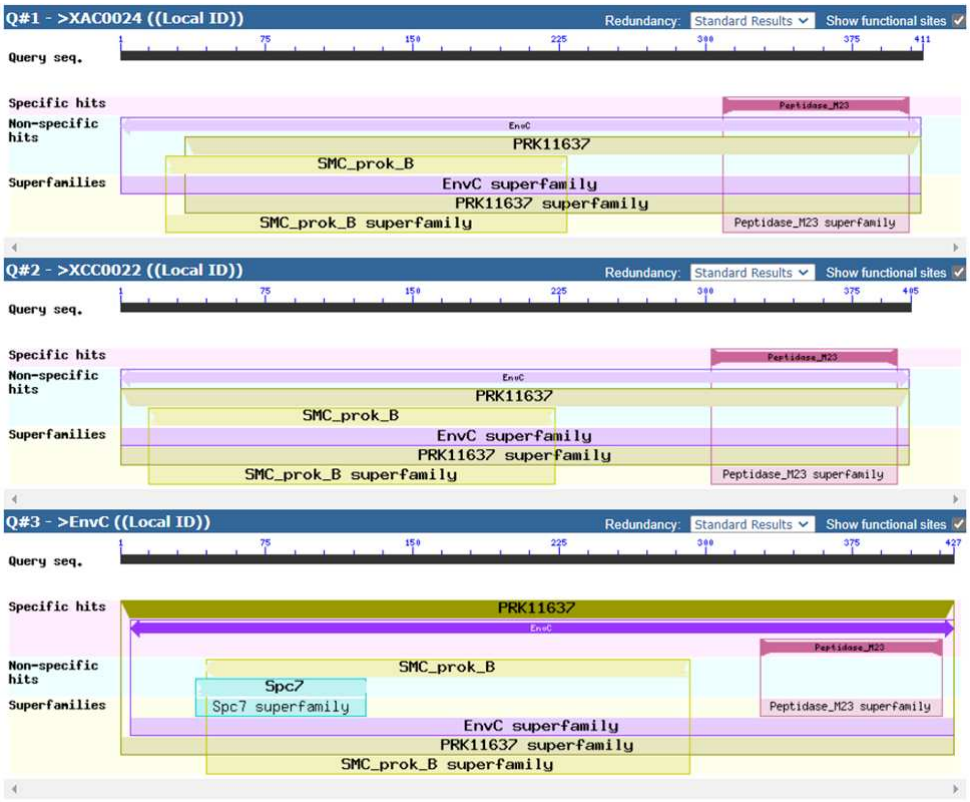

Figure 2. Domain multiple sequence alignment of XAC0024 from *X. citri* 306, XCC0022 from *Xanthomonas campestris* and EnvC from *E. coli* (NC_000913). The protein sequences were uploaded from the NCBI Batch Web CD-Search tool.

In order to reinforce the similarity between the *Xanthomonas* strains sequences used for the phylogeny reconstruction, we utilized the NCBI Batch Web CD-Search tool, which showed the conserved domain peptidase M23 being shared by 16 representative *Xanthomonas* species (Supplementary Figure S5). This observation suggests a potential conserved function for this domain among homologs [35].

As the XAC0024 protein's 3-D structure has not been determined and is unavailable in the Protein Data Bank (PDB), we employed its protein sequence as a query for generating a graphical 3-D molecular model using the I-TASSER server, which was then compared with the known structure of EnvC from *E. coli*. The comparison between the EnvC protein from *E. coli* and XAC0024 from *X. citri* revealed 33% identity and a similarity of 52%, and almost identical 3-D structures (Figure 3 and Supplementary Figure S6). EnvC protein from *E. coli* was shown to be slightly larger than its homolog XAC0024 from *X. citri.*

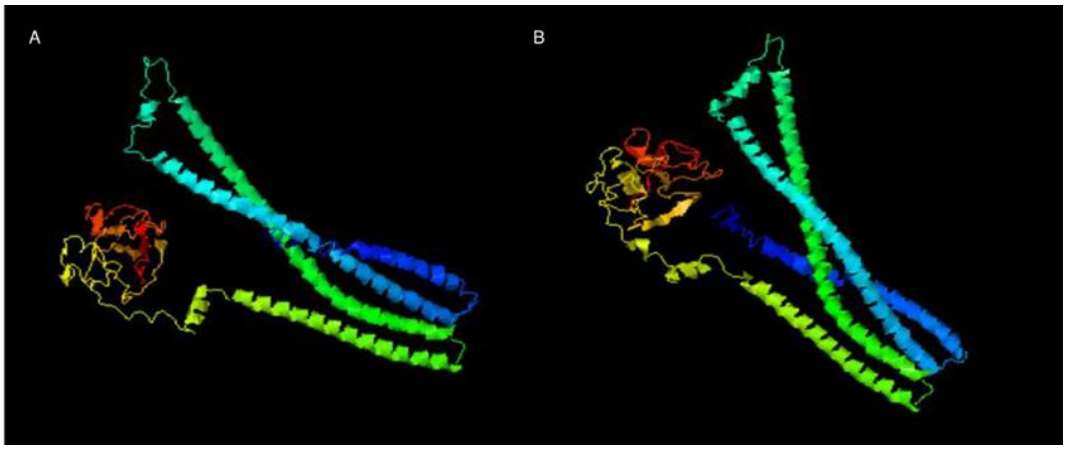

Preprints (www.preprints.org) | NOT PEER-REVIEWED | Posted: 12 October 2023 doi:10.20944/preprints202310.0767.v1

Figure 3. 3-D molecular model of A: EnvC protein (*X. citri*) and B: EnvC protein *(E. coli*) based on the predicted structure performed by I-TASSER server.

3.2. Disruption of envC affects X. citri virulence

To investigate the role of *envC*, we produced an *envC* deletion mutant (Δ*envC*) and assessed its virulence and viability in comparison with the wild-type isolate *X. citri* 306. These analyses involved assessing *in planta* symptomatology and conducting both *in planta* and *in vitro* growth curves. To determine the contribution of EnvC to virulence, Rangpur lime leaves were inoculated with *X. citri* wt, Δ*envC*, and Δ*envC* complemented strain (Δ*envC* pMAJIIc-*envC*) and monitored for 15 days for development of citrus canker symptoms. The chronological development of symptoms showed hypertrophy/hyperplasia, followed by water soaking, and brownish necrosis lesions at the late stage of infection, typical of citrus canker disease, in both *X. citri* wt and Δ*envC* pMAJIIc-*envC* strains. However, the mutant Δ*envC* exhibited a delay in the induction of citrus canker symptoms and produced less severe lesions. These appeared to be concentrated close to the point of inoculation (Figure 4A).

Furthermore, we investigated the contribution of *envC* to host colonization. The population of *X. citri* wt reached its maximal level around 10 days after inoculation, increasing its population by approximately 5,000-fold (Figure 4B). In contrast, the population of Δ*envC* did not show significant change *in planta*, increasing its population less than 10-fold (Figure 4B). This indicates that Δ*envC* was unable to multiply within the plant mesophyll. Subsequently, we examined whether *envC* is essential for cell viability and multiplication by monitoring its growth in NB medium. The results revealed that Δ*envC* displayed an altered growth pattern when compared to *X. citri* wt (Figure 4C). Initially, the mutant displayed an accelerated growth rate; however, Δ*envC* reached a plateau at a significantly lower population than *X. citri* wt and Δ*envC* pMAJIIc-*envC* strains. These results demonstrate that EnvC is required for the virulence of *X. citri* and host colonization, and its disruption affects cell viability and multiplication.

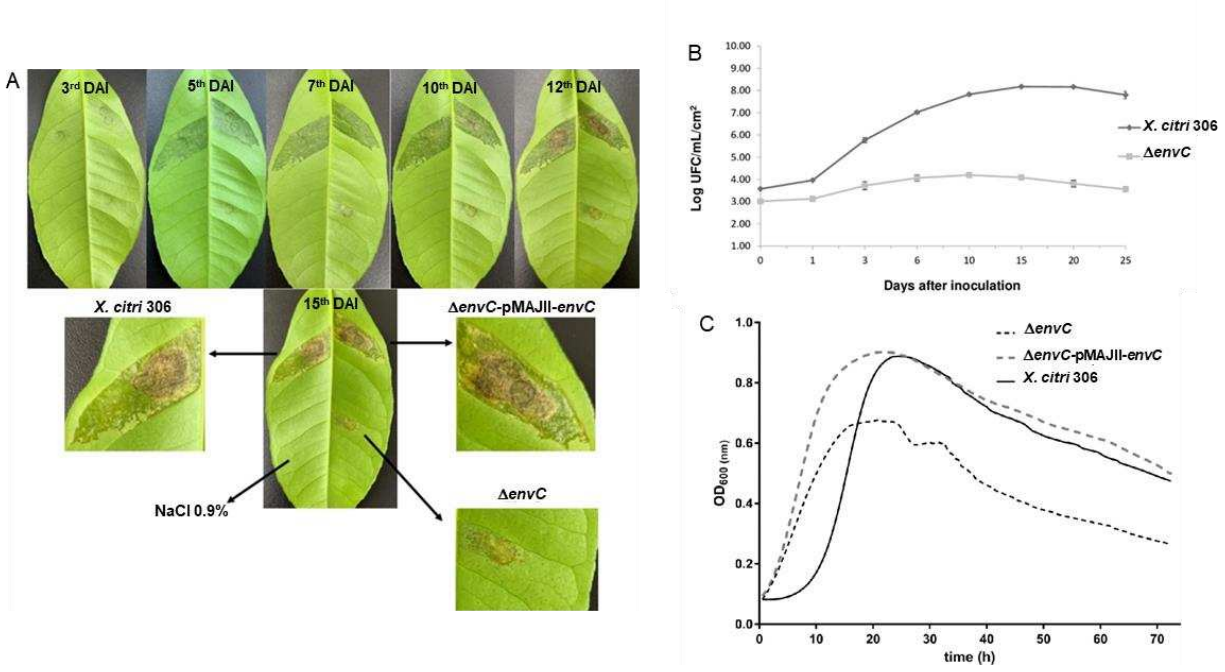

Figure 4. Pathogenicity assay and growth curves for *X. citri* 306, Δ*env*C and Δ*env*C - pMAJIIc-*env*C. A. Rangpur lime leaves were infiltrated with cells suspensions of the indicated *X. citri* strains. Pictures were taken on the 3rd, 5th, 7th, 10th, 12th and 15th days after inoculation (DAI). B: *in planta* growth curve. Leaves of Rangpur lime were infiltrated with cell suspensions of the indicated *X. citri* strains and bacterial populations were quantified at 0, 1, 3, 6, 10, 15, 20 and 25 DAI. C: *in vitro* growth curve. *X. citri* 306, Δ*env*C and Δ*env*C - pMAJIIc-*env*C were cultivated in NB medium and OD_{600nm} reading were taken every 30 min for 72 hours. All the experiments were done in triplicate.

Preprints (www.preprints.org) | NOT PEER-REVIEWED | Posted: 12 October 2023 doi:10.20944/preprints202310.0767.v1

3.3. EnvC is required for X. citri daughter cell separation

To determine the subcellular localization of EnvC encoded by *X. citri*, we expressed a version of the protein as an mCherry fusion (EnvC-mCherry) (Figure 5). *X. citri* EnvC-mCherry expressing cells (pMAJIIc-*envC*) exhibited a strong fluorescence signal primarily concentrated around the edges of the cells, while the cytoplasm remained non-fluorescent (Figure 5B,C). This phenotype suggests that *X. citri* EnvC occupies the periplasmic region of the cells. Importantly, the wild-type *X. citri* strain used as a control showed no fluorescence emission (Figure 5E,F).

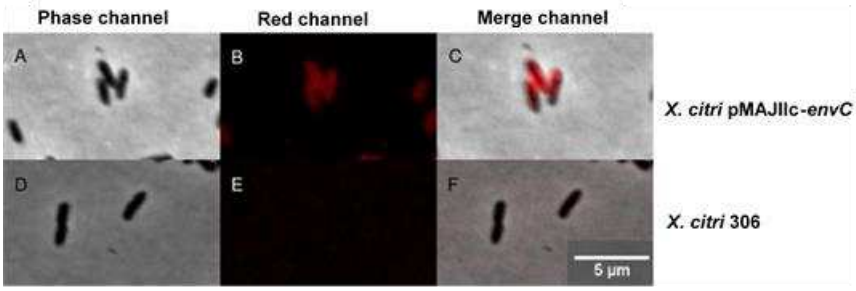

Figure 5. Subcellular localization of EnvC-mCherry in *X. citri*. *X. citri* strain expressing EnvC-mCherry fusions were cultivated until $OD600_{nm}$ of 0.3, and subsequently induced with 0.05% arabinose for 2 hours prior to microscope observation. Panels show the phase contrast (left), TxRed channels (middle) and the overlay, respectively for A-C: *X. citri* pMAJIIc-*env*C, D-F: *X. citri* 306. Magnification 100X; scale bar 5 µm.

Next, we investigated the possible roles of EnvC in cell division and chromosome segregation by examining DAPI-stained *X. citri* wild-type (wt), Δ*envC*, and Δ*envC* pMAJIIc-*envC* cells (Figure 6). The *X. citri* Δ*envC* cells exhibited abnormally shaped rods, somewhat curved (Figure 6 D,F). Many cells were organized in long-chained structures, displaying clear division constrictions, which occasionally gave rise to minicells (Figure 6G,I; arrows). Although Δ*envC* mutants appeared competent in the initial stages of the division process, they exhibited evident and detectable late-division/separation defects.

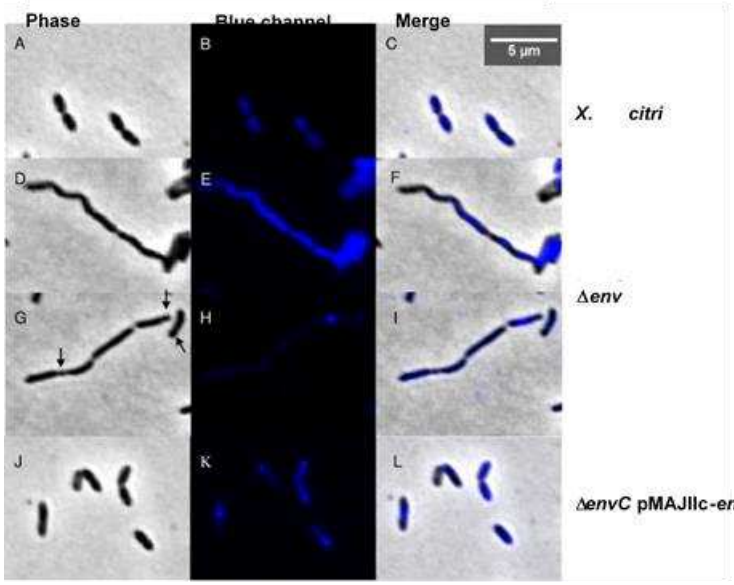

Figure 6. Cell morphology and nucleoid distribution analyses of *X. citri* 306, Δ*env*C and Δ*env*C pMAJIIc-*env*C strains. Panels show the phase contrast (left), DAPI channels (middle) and the overlay, respectively for A-C: *X. citri* 306, D-I: Δ*env*C, H-L: Δ*env*C - pMAJIIc-*env*C. Arrows indicates the minicell position. Magnification 100X; scale bar 5 µm.

For the cells that were not part of a chain, thus displaying an overall normal shape, we observed a significant difference in their average cell length compared to *X. citri* wild-type and Δ*envC* pMAJIIc-

 doi:10.20944/preprints202310.0767.v1

envC strains (Table 2). To quantitatively evaluate this, we measured 400 individual cells from each culture: *X. citri* wild-type, Δ*envC*, and Δ*envC* pMAJIIc-*envC*. *X. citri* wild-type had an average cell length of 1.18 ± 0.22 μm, while Δ*envC* pMAJIIc-*envC* had an average cell length of 1.22 ± 0.29 μm. In contrast, *X. citri* Δ*envC* mutants exhibited an average cell length of 1.89 ± 0.38 μm. Additionally, we scored the percentages of observed abnormalities for *X. citri* Δ*envC* mutants (Table 2), where filamented chains comprised approximately 55.5% of the cells, while minicells accounted for 5.25% (n= 400).

Table 2. Morphological analysis of *X. citri* strains according to cell length.

	Cell length μm	Filaments %	Minicells %
X. citri 306	1.18 ± 0.22[a]	0	0
Δ*envC*	1.89 ± 0.38[b]	55.5	5.25
Δ*envC* pMAJIIc-*envC*	1.22 ± 0.29[a]	0	0

Total *n*= 400 cells measured. Data correspond to the average cell length ± standard deviation. Same letters mean no significant difference according to the *Tukey test* - 0.05.

Chromosome organization was visualized using 4',6-diamidino-2-phenylindole (DAPI)-staining (Figure 6). Cultures of Δ*envC* mutant exhibited a continuous distribution of chromosomal mass spanning through the elongated cells (Figure 6 E,F,H,I). This continuous distribution in some cells possibly hindered septal closure. In contrast, both *X. citri* and Δ*envC* pMAJIIc-*envC* strains displayed a bilobed chromosome organization pattern with the expected normal distribution, indicating successful complementation of the mutant (Figure 6 B,C,K,L). (Figure 6B,C,K,L). In all strains, a strong signal of nucleoid accumulation in the middle or pole of the cells could also be observed (Figure 6B,H,K), consistent with previous observations in the *E. coli* wt strain [36] and *X. citri* 306 wt strain [17].

4. Discussion

The EnvC protein encoded by *Xanthomonas citri* has a predicted M23 peptidase domain, which is part of a superfamily of metallopeptidase, characterized by the presence of zinc in its active enzyme site [37]. This enzyme family includes the Nlpd from *E. coli*, a LytM factor responsible, as well as EnvC, for activating N-acetylmuramoyl-L-alanine amidases (AmiA, AmiB and AmiC). These amidases play a crucial role in daughter cell separation, and the inactivation of the genes that encode them results in long cell chains formation [38,7,8].

In this study, we demonstrated the *envC* mutant of *Xanthomonas citri* strain displayed a defect in cell separation, accompanied by distinct changes in cell morphology. Cultures of Δ*envC* mutant exhibited elongated rods, long-chained cells and minicells, which indicated impaired daughter cell separation. These findings are consistent with results previously reported in *X. campestris* strains lacking *nlpD*, *envC* or *amiC1* [13], which also exhibited severe defects in daughter cell separation. The physiological roles of peptidoglycan hydrolases, including EnvC, are still not fully understood, as the loss of an individual enzyme has little effect on growth and division, suggesting functional overlap between numerous hydrolases [2]. To shed light on EnvC's specific role, a collection of *E. coli* mutants lacking individual LytM factors (EnvC, NlpD, YgeR and YebA), as well as all possible combinations of them, were previously analyzed [7]. Among these mutants, only those with *envC* deletion failed to separate normally, further confirming the critical role of EnvC in proper cell separation.

Our observations of chromosome segregation errors in the *X. citri* Δ*envC* mutant suggest that they are linked to the delayed division induced by the absence of EnvC. Interestingly, complementation of the mutant with *X. citri* Δ*envC* pMAJIIc-*envC* restored a normal phenotype, with no detectable morphological discrepancies compared to the wild-type strain. Although further investigation is warranted, these results indicate that the Δ*envC* mutant indeed experiences a late-division/separation defect, possibly leading to longer cell compartments and allowing the chromosomal mass to span across.

 doi:10.20944/preprints202310.0767.v1

The *X. citri* mutant lacking *envC* exhibited a delay in citrus canker symptomatology compared with the wt and complemented strains. This delay in symptom development demonstrated that the deletion of EnvC had a significant impact on the bacteria's virulence, as evidenced by its reduced ability to induce symptoms when inoculated into citrus leaves, which are susceptible hosts. The complemented strain, Δ*envC* pMAJIIc-*envC*, fully restored virulence, confirming that the phenotype observed in the Δ*envC* mutant was specifically due to the absence of EnvC and not a result of a polar mutation.

Interestingly, *Xanthomonas campestris* strains lacking either *nlpD* or *amiC1* almost completely lost its virulence, but the mutant lacking *envC* showed levels of virulence compared to the wt strain [13]. This indicates that the contribution of EnvC to virulence is species-specific and that EnvC may be directly or indirectly involved in specific virulence pathways that differ between *Xanthomonas* strains. The species-specific role of EnvC in virulence highlights the complex and intricate nature of bacterial pathogenesis, where different strains of the same genus may employ distinct mechanisms to establish disease. Further investigations into the specific pathways influenced by EnvC in different *Xanthomonas* strains could provide valuable insights into the molecular basis of pathogenicity and potential targets for disease control strategies.

According to the amino acid sequence analysis performed by SignalP 5.0 server [39], EnvC from *Xanthomonas citri*, *E. coli*, and *Xanthomonas campestris* possesses a signal peptide with specific cleavage sites (Supplementary Figure S7). The cleavage site for EnvC in *Xanthomonas citri* is between amino acids 20 and 21 (Figure S7A), while for *E. coli*, it is between amino acids 42 and 43, and for *Xanthomonas campestris*, it is between amino acids 14 and 15 (Figure S7B,C). The presence of the signal peptide, which can serve as a membrane anchor, suggests that EnvC proteins are likely to be transported to the periplasmic region, a common localization for proteins in many pathogenic bacteria, often facilitated by tat/sec systems in gram-negative bacteria [40, 41, 42, 43, 44, 45, 46, 47]. The localization pattern observed here for EnvC-mCherry fusion protein in *Xanthomonas citri* and *E. coli* [7] are consistent with the fusion protein occupying the periplasmic region of the bacterium [17]. This subcellular localization supports the notion that EnvC functions in the periplasm, where it may play a crucial role in late-division and daughter cell separation processes, as supported by similar findings in other bacterial models [6, 7, 12, 46].

Taken together, our results, as well as similar results from many other bacterial models, support the notion that EnvC has a function in late-division and daughter cell separation [6, 7, 12, 46]. However, the mechanism by which *X. citri* EnvC operates on daughter cell separation, considering its periplasmic location, and how and if this protein interacts with other hydrolases are intriguing questions that warrant further exploration and investigation.

Supplementary Materials: The following supporting information can be downloaded at: www.mdpi.com/xxx/s1, Figure S1: Deletion of the central portion of gene XAC0024 from *X. citri* by double-joint PCR; Figure S2: Nucleotide sequence alignment between XAC0024 from *Xanthomonas citri* and its homologue XCC0022 from *Xanthomonas campestris*; Figure S3: Protein sequence alignment between XAC0024 from *Xanthomonas citri* and its homologue XCC0022 from *Xanthomonas campestris*; Figure S4: Domain multiple sequence alignment of the nine ORFs of *X. citri* sharing the M23 domain; Figure S5: Domain multiple sequence alignment of 16 representative species within the *Xanthomonas* species used in the Maximum Likelihood phylogeny; Figure S6: Protein sequence alignment between XAC0024 from *Xanthomonas citri* and EnvC from E. *coli*; Table S1: Proteins of *Xanthomonas citri* subsp. *citri* 306 strain sharing the Peptidase M23 Domain according to an *in-silico* search using the IMG 'find function' tool; Table S2: Primers used in this study; Table S3: ; Table S1 ; Table S1 ; Table S1

Author Contributions: Conceptualization, Michelle M. Pena, Henrique Ferreira and Jesus A. Ferro; Formal analysis, Michelle M. Pena, Thaisa Z. Martins and Doron Teper; Funding acquisition, Nian Wang, Maria Inês T. Ferro and Jesus A. Ferro; Investigation, Michelle M. Pena, Thaisa Z. Martins, Doron Teper, Caio Zamuner, Helen Penha and Henrique Ferreira; Methodology, Michelle M. Pena, Thaisa Z. Martins, Henrique Ferreira and Jesus A. Ferro; Project administration, Michelle M. Pena and Jesus A. Ferro; Resources, Nian Wang and Maria Inês T. Ferro; Supervision, Henrique Ferreira, Nian Wang and Jesus A. Ferro; Validation, Michelle M. Pena and Jesus A. Ferro; Visualization, Michelle M. Pena and Jesus A. Ferro; Writing – original draft, Michelle M. Pena; Writing – review & editing, Michelle M. Pena, Doron Teper, Henrique Ferreira, Nian Wang and Jesus A. Ferro All authors have read and agreed to the published version of the manuscript.

Funding: This work is part of the Ph.D. thesis of M. M. Pena and master's dissertation of T. Z. Martins and was financed in part by the Coordenação de Aperfeiçoamento de Pessoal de Nível Superior – Brasil (CAPES) – Finance Code 001 and by a fellowship grant from Conselho Nacional de Desenvolvimento Científico e Tecnológico – Brasil (CNPq) to JAF (Grant No. 312089/2019-8). M.I.T.F. is a recipient of a CNPq productivity fellowship (XXXX).

Data Availability Statement: Not applicable.

Acknowledgments: We thank Citrus Research and Education Center from the University of Florida for allowed to use their microscope facilities. We also thank Naiara Zancanari for the support with analyzes and the Sequencing Facility of the Center for Biological Resources and Genomic Biology (CREBIO) from the University of São Paulo State (UNESP) at Jaboticabal Campus, Brazil.

Conflicts of Interest: The authors declare no conflict of interest. The funders had no role in the design of the study; in the collection, analyses, or interpretation of data; in the writing of the manuscript; or in the decision to publish the results.

References

1. DAS, A.K. Citrus Canker - A review. *J. Appl. Hortic*. **2003**, *5*, 52-60. doi: 10.37855/jah.2003.v05i01.15.
2. Vollmer, W.; Blanot, D.; de Pedro, M. A. Peptidoglycan structure and architecture. *FEMS Microbiol. Rev*. **2008**, *32*, 149-167. doi: 10.1111/j.1574-6976.2007.00094.x.
3. Silhavy, T.J.; Kahne, D.; Walker, S. The bacterial cell envelope. *Cold Spring Harb. Perspect. Biol.* **2010**, *2*, a000414. doi: 10.1101/cshperspect.a000414.
4. Frirdich, E.; Gaynor, E.C. Peptidoglycan hydrolases, bacterial shape, and pathogenesis. *Curr. Opin. Microbiol*. **2013**, *16*, 767-778. doi: 10.1016/j.mib.2013.09.005.
5. Firczuk, M.; Bochtler, M. Folds and activities of peptidoglycan amidases. *FEMS Microbiol. Rev*. **2007**, *31*, 676-691. doi: 10.1111/j.1574-6976.2007.00084.x.
6. Bernhardt, T.G.; de Boer, P.A. The *Escherichia coli* amidase AmiC is a periplasmic septal ring component exported via the twin-arginine transport pathway. *Mol. Microbiol*. **2003**, *5*, 1171–1182. doi: 10.1046/j.1365-2958.2003.03511.x.
7. Uehara, T.; Dinh, T.; Bernhardt, T.G. LytM-domain factors are required for daughter cell separation and rapid ampicillin-induced lysis in *Escherichia coli*. *J. Bacteriol*. **2009**, *191*, 5094-5107. doi: 10.1128/JB.00505-09.
8. Uehara, T.; Parzych, K.R.; Dinh, T.; Bernhardt, T G. Daughter cell separation is controlled by cytokinetic ring-activated cell wall hydrolysis. *EMBO J*. **2010**, 29, 1412-1422. doi: 10.1038/emboj.2010.36.
9. Wu, C.; Al Mamun A.A.M.; Luong, T.T., Hu, B.; Gu, J.; Lee, J.H.; D'Amore, M.; Das A.; Ton-That, H. Forward Genetic Dissection of Biofilm Development by Fusobacterium nucleatum: Novel Functions of Cell Division Proteins FtsX and EnvC. *mBio*, **2018,** 9, e00360-18. doi: 10.1128/mBio.00360-18.
10. Möll, A.; Dörr, T.; Alvarez, L.; Chao, M.C.; Davis, B.M.; Cava, F.; Waldor, M.K. Cell separation in Vibrio cholerae is mediated by a single amidase whose action is modulated by two nonredundant activators. *J. Bacteriol.* **2014**, 196, 3937-3948. doi: 10.1128/JB.02094-14.
11. Warr, A.R.; Hubbard, T.P.; Munera, D.; Blondel, C.; Wiesch, P.Az; Abel. S.; Wang, X.; Davis, B.M.; Waldor, M.K. Transposon-insertion sequencing screens unveil requirements for EHEC growth and intestinal colonization. *PLoS Pathog*. **2019**, 15, e1007652. doi: 10.1371/journal.ppat.1007652.
12. Yakhnina, A.A.; Mcmanus, H.R.; Bernhardt, T.G. The cell wall amidase AmiB is essential for Pseudomonas aeruginosa cell division, drug resistance and viability. Mol. Microbiol. **2015**, 97, 957-973. doi: 10.1111/mmi.13077.
13. Yang, L.C., Gan, Y.L.; Yang, L.Y.; Jiang, B.L.; Tang, J.L. Peptidoglycan hydrolysis mediated by the amidase AmiC and its LytM activator NlpD is critical for cell separation and virulence in the phytopathogen *Xanthomonas campestris*. *Mol. Plant Pathol*. **2018**, *19*, 1705-1718. doi: 10.1111/mpp.12653.
14. Sambrook, J.; Fritsch, E.R.; Maniatis, T. *Molecular Cloning: A Laboratory Manual*, 2nd ed.; Cold Spring Harbor Laboratory Press: New York, NY, USA, 1989, Volume 1.
15. da Silva, A.C.; Ferro, J.A.; Reinach, F.C.; Farah, C.S.; Furlan, L.R.; Quaggio, R.B.; Monteiro-Vitorello, C.B.; Van Sluys, M.A.; Almeida, N.F.; Alves, L.M.; et al. Comparison of the genomes of two *Xanthomonas* pathogens with differing host specificities. *Nature* **2002**, *417*, 459–463. doi: 10.1038/417459a.
16. Huguet, E.; Hahn, K.; Wengelnik, K.; Bonas, U. hpaA mutants of *Xanthomonas campestris* pv. *vesicatoria* are affected in pathogenicity but retain the ability to induce host-specific hypersensitive reaction. *Mol. Microbiol*. **1998**, *29*, 1379-1390. doi: 10.1046/j.1365-2958.1998.01019.x
17. Pena, M.M.; Teper, D.; Ferreira, H.; Wang, N.; Sato, K.U.; Ferro, M.I.T.; Ferro, J.A. mCherry fusions enable the subcellular localization of periplasmic and cytoplasmic proteins in *Xanthomonas* sp. PLoS ONE **2020**, *15*, e0236185. doi: 10.1371/journal.pone.0236185.
18. Lee, J.; Lee, H-J.; Shin, M-K.; Ryu, W-S. Versatile PCR-mediated insertion or
1. deletion mutagenesis. *BioTechniques* **2004**, *36*, 398-400. doi: 10.2144/04363BM04.

19. do Amaral, A.M.; Toledo, C.P.; Baptista, J.C.; Machado, M.A. Transformation of *Xanthomonas axonopodis* pv. citri by electroporation. *Fitopatol. Bras.* **2005**, *30*, 292–294. doi:10.1590/S0100-41582005000300013.
20. Kaniga, K.; Delor, I.; Cornelis, G.R. A wide-host-range suicide vector for improving reverse genetics in Gram-negative bacteria: inactivation of the *bla*A gene of *Yersinia enterocolitica*. *Gene* **1991**, *109*, 137-141. doi: 10.1016/0378-1119(91)90599-7.
21. Martins, P.M.M.; Lau, I.F.; Bacci, Jr.M.; Belasque, J.; Do Amaral, A.M.; Taboga, S. R.; Ferreira, H. Subcellular localization of proteins labeled with GFP in *Xanthomonas citri* ssp. *citri*: targeting the division septum. *FEMS Microbiol. Lett*. **2010**, *310*, 76-83. doi:10.1111/j.1574-6968.2010.02047.x.
22. Morão, L.G.; Polaquini, C.R.; Kopacz, M.; Torrezan, G.S.; Ayusso, G.M.; Dilarri, G.; Cavalca, L.B.; Zielinska, A.; Scheffers, D-J.; Regasini, L.O.; Ferreira, H. A simplified curcumin targets the membrane of *Bacillus subtilis*. *MicrobiologyOpen* **2019**, *8*, e683. doi: 10.1002/mbo3.683.
23. LACERDA, L.A.; CAVALCA, L.B.; MARTINS, P.M.M.; GOVONE, J.S.; BACCI, JR.M.; FERREIRA, H. Protein depletion using the arabinose promoter in *Xanthomonas citri* subsp. *citri*. *Plasmid* **2017**, *90*, 44-52. doi: 10.1016/j.plasmid.2017.03.005.
24. Thompson, J.D.; Higgins, D.G.; Gibson, T.J. CLUSTAL W: improving the sensitivity of progressive multiple sequence alignment through sequence weighting, positions-specific gap penalties and weight matrix choice. *Nucleic Acids Res.***1994**, *22*, 4673 - 4680. **doi: 10.1093/nar/22.22.4673.**
25. Miller, M.A.; Pfeiffer, W.; Schwartz, T. Creating the CIPRES Science Gateway for Inference of Large Phylogenetic Trees. *Proceedings of the Gateway Computing Environments Workshop* **2010**, 14, 1-8. doi: 10.1109/GCE.2010.5676129.
26. Stamatakis, A. RAxML Version 8: A tool for phylogenetic analysis and post-analysis of large phylogenies. *Bioinformatics* **2014**, 30, 1312-1313. doi: 10.1093/bioinformatics/btu033.
27. Felsenstein, J. Confidence limits on phylogenies: an approach using the bootstrap. *Evolution* **1985**, 39, 783-791. doi: 10.2307/2408678.
28. KUMAR, S.; STECHER, G.; LI, M.; KNYAZ, C.; TAMURA, K. MEGA X: molecular evolutionary genetics analysis across computing platforms. *Mol. Biol. Evol.* **2018**, 35, 1547-1549. doi: 10.1093/molbev/msy096.
29. Yang, J.; Yan, R., Roy, A.; Xu, D.; Poisson, J.; Zhang, Y. The I-TASSER Suite: Protein structure and function prediction. *Nat. Methods* **2015**, 12, 7-8. doi: 10.1038/nmeth.3213.
30. The Xanthomonas sp. Portal – INRA. Available online: https://iant.toulouse.inra.fr/bacteria/annotation/cgi/xansp.cgi (accessed on 24 July 2023).
31. The National Center for Biotechnology Information – NCBI. https://www.ncbi.nlm.nih.gov/search/all/?term=WP_053884339 (accessed on 24 July 2023).
32. Timilsina, S.; Potnis, N.; Newberry; E.A. *et al. Xanthomonas* diversity, virulence and plant–pathogen interactions. *Nat. Rev. Microbiol.* **2020**, 18, 415–427. doi: 10.1038/s41579-020-0361-8.
33. Rodriguez-R, L.M.; Grajales, A.; Arrieta-Ortiz, M.L.; Salazar, C.; Restrepo, S.; Bernal, A. Genomes-based phylogeny of the genus *Xanthomonas*. *BMC Microbiol*. **2012**, 12:43. doi: 10.1186/1471-2180-12-43.
34. Timilsina, S.; Kara, S.; Jacques, M.A.; Potnis, N.; Minsavage, G.V.; Vallad, G.E.; Jones, J.B.; Fischer-Le Saux, M. Reclassification of *Xanthomonas gardneri* (ex Šutič 1957) Jones *et al.* 2006 as a later heterotypic synonym of *Xanthomonas cynarae* Trébaol *et al.* 2000 and description of *X. cynarae* pv. *cynarae* and *X. cynarae* pv. *gardneri* based on whole genome analyses. *Int. J. Syst. Evol. Microbiol*. **2019**, 69, 343-349. doi: 10.1099/ijsem.0.003104.
35. Altenhoff, A.M.; Studer, R.A.; Robinson-Rechavi, M.; Dessimoz, C. Resolving the ortholog conjecture: orthologs tend to be weakly, but significantly, more similar in function than paralogs. *PLoS Comput. Biol*. **2012**, 8, e1002514. doi: 10.1371/journal.pcbi.1002514.
36. Freiesleben, U.V.; Krekling, M.A.; Hansen, F.G.; Lobner-Olesen, A. The eclipse period of *Escherichia coli*. *The EMBO Journal* **2000**, 19, 6240-6248. doi: 10.1093/emboj/19.22.6240.
37. Wu, Q.; Lahti, J.M.; Air, G.M.; Burrows, P.D.; Cooper, M.D. Molecular cloning of the murine BP-1/6C3 antigen: a member of the zinc-dependent metallopeptidase family. *Proc. Natl. Acad. Sci. U.S.A*. **1990**, *87*, 993-997. doi: 10.1073/pnas.87.3.993.
38. Heidrich, C.; Templin, M.F.; Ursinus, A.; Merdanovic, M.; Berger, J.; SCHWARZ, H.; de Pedro, M.A.; Holtje, J.V. Involvement of N-acetylmuramyl-L-alanine amidases in cell separation and antibiotic-induced autolysis of *Escherichia coli*. *Mol. Microbiol*. **2001**, 41, 167-178. doi: 10.1046/j.1365-2958.2001.02499.x.
39. Armenteros, J.J.A.; Tsirigos, K.D.; Sonderby, C.K.; Peterson, T.N.; Winther, O.; Brunak, S.; Heijne, G.V.; Nielsen, H. SignalP 5.0 improves signal peptide predictions using deep neural networks. *Nat. Biotechnol.* **2019**, 37, 420-423. doi: 10.1038/s41587-019-0036-z.
40. Brunings, A.M.; Gabriel, D.W. *Xanthomonas citri*: breaking the surface. *Mol. Plant Pathol.* **2003**, 4, 141-157. doi:10.1046/j.1364-3703.2003.00163.x.
41. Jha, G.; Rajeshwari, R.; Sonti, R.V. Bacterial Type Two Secretion System Secreted Proteins: Double-Edged Swords for Plant Pathogens. *Mol. Plant Microbe Interact.* **2005**, 18,891-898. doi: 10.1094/MPMI-18-0891
42. Büttner, D.; Bonas, U. Regulation and secretion of *Xanthomonas* virulence factors. *FEMS Microbiol. Rev.* 2010, 34, 107-133, **2010**. doi: 10.1111/j.1574-6976.2009.00192.x.

43. Soares, M.R.; Facincani, A.P.; Ferreira, R.M.; Moreira, L.M.; DE Oliveira, J.C. F.; Ferro, J.A.; Ferro, M.I.T.; Meneghini, R.; Gozzo, F.C. Proteome of the phytopathogen *Xanthomonas citri* subsp. *citri*: a global expression profile. *Proteome Sci.* **2010**, 8: 55. doi: 10.1186/1477-5956-8-55.
44. Ryan, R.P.; Vorhölter, F.J.; Potnis, N.; Jones, J.B.; Sluys, M-A.V.; Bogdanove, A.J.; Dow, J.M. Pathogenomics of *Xanthomonas*: understanding bacterium–plant interactions. *Nat. Rev. Microbiol.* **2011**, 9, 344-355. doi: 10.1038/nrmicro2558.
45. Yan, Q.; Wang, N. The ColR/ColS two-component system plays multiple roles in the pathogenicity of the citrus canker pathogen *Xanthomonas citri* subsp. *citri*. *J. Bacteriol*. **2011**, 193, 1590-1599. doi: 10.1128/JB.01415-10.
46. Zimaro, T.; Thomas, L.; Marondedze, C.; Sgro, G.G.; Garofalo, C.G.; Ficarra, F.A.; Gehring, C.; Ottado, J.; Gottig, N. The type III protein secretion system contributes to *Xanthomonas citri* subsp. *citri* biofilm formation. *BMC Microbiol*. **2014**, 14:96. doi: 10.1186/1471-2180-14-96.
47. Zhou, X.; Hu, X.; Li, J.; Wang, N. A Novel Periplasmic Protein, VrpA, Contributes to Efficient Protein Secretion by the Type III Secretion System in *Xanthomonas* spp. *Mol. Plant Microbe Interact*. **2015**, 28, 143-153. doi: 10.1094/MPMI-10-14-0309-R.